Journal of Theoretical Biology 435 (2017) 98–105

Contents lists available at ScienceDirect

Journal of Theoretical Biology

journal homepage: www.elsevier.com/locate/jtbi

Inter-airway structural heterogeneity interacts with dynamic heterogeneity to determine lung function and flow patterns in both asthmatic and control simulated lungs

G.M. Donovan

Department of Mathematics, University of Auckland, New Zealand

ARTICLE INFO

Article history:
Received 1 June 2017
Revised 23 August 2017
Accepted 28 August 2017
Available online 1 September 2017

Keywords:
Airway dynamic
Ventilation heterogeneity
Clustered ventilation defects

ABSTRACT

Asthma is a disease involving both airway remodelling (e.g. thickening of the airway wall) and acute, reversible airway narrowing driven by airway smooth muscle contraction. Both of these processes are known to be heterogeneous, and in this study we consider a new theoretical model which considers the interactions of both mechanisms: structural heterogeneity (variation in airway remodelling) and dynamic heterogeneity (emergent variation in airway narrowing and flow). By integrating both types of inter-airway heterogeneity in a full human lung geometry, we are able to draw several insights regarding the mechanisms underlying observed ventilation heterogeneity. We show that: (1) bimodal ventilation distributions are driven by paradoxical contraction/dilation patterns for airways of all sizes; (2) structural heterogeneity differences between asthmatic and control subjects significantly influences resulting lung function, and observed ventilation heterogeneity patterns; and (3) individual airway dilation probabilities are uncorrelated with prior airway remodelling of that airway.

1. Introduction

Asthma is a widespread disease which fundamentally involves both reversible airway narrowing and airway remodelling (irreversible, or at least reversible only on a much slower timescale). However, the underlying biological processes driving excessive narrowing and/or remodelling in asthma are not well understood. For most sufferers of asthma, symptoms can be reasonably well controlled using some combination of the standard suite of therapies; however, a minority, whose symptoms are not well controlled by existing treatments, present significant challenges. It is here that our lack of fundamental understanding of the underlying biological processes presents a barrier to understanding the shortcomings of existing therapies for this minority of patients, and in developing new treatments.

For example, heterogeneity is thought to be important in determining lung function, yet poorly understood. Ventilation heterogeneity has been observed by many groups, using different imaging modalities (e.g. Layachi et al. (2013); Lui et al. (2015); Tzeng et al. (2009)). One example using hyperpolarized helium-3 MRI in both healthy and asthmatic subjects is given in Fig. 1. It has long been understood that heterogeneity of airway properties (e.g. airway wall thickness, airway smooth muscle mass, etc., which we refer to as *structural* heterogeneity) can play an important role in determining lung function (Lutchen and Gillis, 1997; Thorpe and Bates, 1997). These studies employed theoretical models which treated airways as isolated (rather than interconnected) units, and made general assumptions about the distributions of structural heterogeneity (in the absence of specific experimental data at that time), yet showed clearly the potential for heterogeneity of airway properties to be important in determining function. Perhaps equally important is the potential for *dynamic* heterogeneity to emerge, even from homogeneous domains (Anafi and Wilson, 2001; Donovan, 2016b; Donovan and Kritter, 2015; Venegas et al., 2005b). That is, heterogeneous flow patterns can emerge in (model) lungs which are structurally homogeneous, by way of airway-airway interdependence and flow compensation mechanisms (e.g. the Anafi–Wilson instability (Anafi and Wilson, 2001)). However, little has been done to study the potential interaction between structural and dynamic heterogeneity.[1]

In this study we consider how interactions between structural and dynamic heterogeneity give rise to observed ventilation heterogeneity. The dynamic heterogeneity component is based on the ideas of Venegas et al. (2005b), Donovan (2016b) and Anafi and

[1] One notable exception is the work of Leary et al. (2014) who considered dynamic heterogeneity in asymmetric trees; however, they did not consider variation in any other airway properties.

E-mail address: g.donovan@auckland.ac.nz

http://dx.doi.org/10.1016/j.jtbi.2017.08.024
0022-5193/

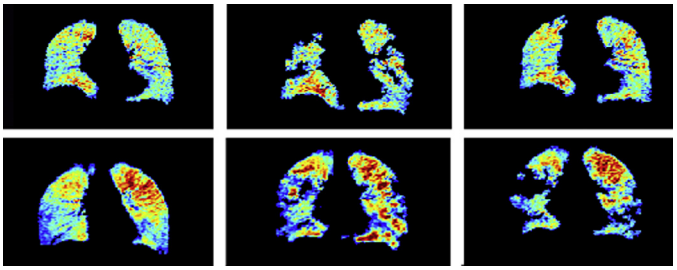

Fig. 1. Quantification of ventilation heterogeneity from hyperpolarized helium-3 MRI. From left to right, top to bottom: healthy pre-challenge; healthy post-challenge; healthy post-deep inspiration (DI); asthmatic pre-challenge; asthmatic post-challenge; asthmatic post-DI. Reproduced from Lui et al. (2015).

Wilson (2001), but extended here to a full human lung; the structural heterogeneity aspect is based on recent experimental data collected from human tissue from both asthmatic and non-asthmatic lungs (Pascoe et al., 2017). This extends previous work which considered the impact of structural heterogeneity on function in non-interacting airway models (Lutchen and Gillis, 1997; Pascoe et al., 2017; Thorpe and Bates, 1997); interacting airway models on homogeneous domains (Donovan and Kritter, 2015; Venegas et al., 2005b); and recent efforts to address both structural heterogeneity and airway interactions simultaneously, albeit on limited domains (Donovan, 2016b; Stewart and Jensen, 2015).[2] By considering interactions between structural heterogeneity, as derived from human tissue histology, and dynamic heterogeneity due to airway interactions/interdependence, on a whole-lung scale, we are able to obtain several important results, both in terms of recapitulating key experimental insights, but also predictive insights which will only become directly testable with imaging advances expected in the coming years. Specifically, we show:

- It is now possible to consider simultaneously both structural and dynamic heterogeneity on a whole human lung scale ($30,000+$ airways), given an appropriate formulation and sufficient attention to details of computational efficiency.
- Variations in structural heterogeneity between control and asthmatic lungs significantly impact both function and ventilation distributions in simulated human lungs.
- Simulated lungs, both control and asthmatic, uniformly exhibit both airway contraction and dilation in response to agonist challenge (long believed theoretically (Venegas et al., 2005b) and recently shown experimentally (Dubsky et al., 2017)). This "paradoxical dilation" or "mixed contraction-dilation pattern" is more pronounced in the smaller airways, but present at all airway sizes, and emphasizes the importance of considering the lung as an entire interconnected system rather than a collection of independent units (Tgavalekos et al., 2007).
- The probability of "paradoxical" dilation of any single airway is independent of the structural remodelling properties of that airway; this is true at all airway sizes, in agreement with recent experimental findings (Dubsky et al., 2017). However it remains likely remodelling properties of the airway tree as a whole are important determinants of contraction-dilation patterns.

2. Model

2.1. Airway tree dynamics

The model of airway tree dynamics used here is based on that of Donovan (2016b), in turn developed from Donovan and Kritter (2015), Venegas et al. (2005b) and Anafi and Wilson (2001). That model is based on synthetic airway trees at sub-lung scale; here we describe the necessary extensions for simulating and analysing behaviour in a full human lung geometry.

Here it is our intent only to briefly overview the model of Donovan (2016b), such as is necessary to explain the modifications employed here. For full details the reader is referred to Donovan (2016b). A brief synopsis of the original differential-algebraic equation (DAE) formulation follows to make clear the changes employed in this study (for extension to full anatomical lung geometry).

Briefly, the model derivation proceeds by describing individual airway dynamics with one ODE per airway; conservation laws governing flow add algebraic constraints giving a system of differential-algebraic equations (DAEs). For a full human lung, the dimensionality is roughly 30,000 variables (one per airway). Coupling (and hence inter-airway interactions) arise via two mechanisms: (1) tethering dependence, in which the tissue mechanical properties depend on flow through the airways (Donovan and Kritter, 2015); and (2) airway-airway coupling via flow conservation and pressure balance (Donovan, 2016b). Fortunately, it is not necessary to deal directly with the system of DAEs, because the structure of the equations allows systematic elimination of the algebraic constraints, reducing the model to a system of ordinary differential equations (ODEs).

Writing $\boldsymbol{r}$ for the vector of airway luminal radii, and $\boldsymbol{p}$ and $\boldsymbol{q}$ for pressures and flows respectively, for the ith airway we have

$$\dot{r}_i = \rho\left(\boldsymbol{\phi}(r_i; \boldsymbol{r}, \boldsymbol{p}, \boldsymbol{q}) - r_i\right) \tag{1}$$

where ρ sets the airway relaxation timescale and the overdot indicates the derivative with respect to time; ϕ describes static airway behaviour, e.g. $\phi = R(P_{tm}(r))$ by composition. $R(P_{tm})$ describes airway radius as a function of transmural pressure according to

$$R(P_{tm}) = \begin{cases} \sqrt{R_i^2(1 - P_{tm}/P_A)^{-n_A}}, & P_{tm} \le 0 \\ \sqrt{r_{imax}^2 - (r_{imax}^2 - R_i^2)(1 - P_{tm}/P_B)^{-n_B}}, & P_{tm} > 0 \end{cases} \tag{2}$$

commonly known as the Lambert model (Lambert et al., 1982). The parameters of Eq. (2) are order dependent and values are given in Donovan (2016b). Here $P(r)$ gives transmural pressure as a function of the radius as

$$P_{tm}(r_i) = p_{mid_i} - \frac{\kappa R_{ref}}{r_i} + \tau(r_i). \tag{3}$$

The second and third terms on the right-hand side are the airway smooth muscle (ASM) and *parenchymal tethering* pressures, respectively. The former includes the ASM activation parameter κ, and a $\propto r^{-1}$ dependence arising from the law of Laplace.[3] The latter arises from the restoring forces generated by the parenchymal tissue surrounding the airway, and is described by

$$\tau(r_i) = 2\mu_i\left(\left(\frac{R_{ref} - r_i}{R_{ref}}\right) + 1.5\left(\frac{R_{ref} - r_i}{R_{ref}}\right)^2\right) \tag{4}$$

according to Lai-Fook (1979), where μ is the parenchymal shear modulus, which crucially *is dependent on lung inflation*. This provides coupling via the parenchymal interdependence. The parameter p_{mid_i} is the mid-airway pressure, and R_{ref} is the reference radius, both as in ref. Donovan (2016b).

For flow through the conducting airways, the conservation constraints are

$$q_m = q_{d_1} + q_{d_2} \tag{5}$$

where the notation here indicates the mother and two daughter branches at each junction. Then in each airway, we assume

[2] Related theoretical models which are not directly connected to this lineage are discussed in Section 4.

[3] See Section 4 for discussion of alternate airway models.

Poiseuille flow

$$\Delta p_i = \alpha_i r_i^{-4} q_i \tag{6}$$

where the constants α_i absorb all dependencies aside from radius, pressure and flow (see Appendix A and Donovan (2016b)). After eliminating the algebraic constraints (details of which are given in Donovan (2016b)), in general form we then have a first order system of ODEs for the airway luminal radii

$$\frac{d\vec{r}}{dt} = f(\vec{r}; \vec{C}) \tag{7}$$

where $\vec{r}$ are the luminal radii, $\vec{C}$ contains the structural airway parameters, and the function f now contains not just the original airway dynamics but now also incorporates the (eliminated) algebraic constraints.[4] From this basis, the following modifications are employed:

1. For the respiratory bronchioles, as in Donovan and Kritter (2015) and Donovan (2016b) we use the local effect that the shear modulus is a function of the local inflation via mean local flow, so that

$$2\mu_i = 0.7 \times \frac{A}{3}\left(|q_i| + |q_{i_{n_1}}| + |q_{i_{n_2}}|\right) \tag{8}$$

   where the parameter A represents the coupling strength and $q_{i_{n_1}}$ and $q_{i_{n_2}}$ are flows in the two nearest respiratory bronchioles.[5] The central idea is that the elastic recoil of the surrounding parenchyma, transmitted by the parenchymal attachments, depends on the inflation of that tissue. The previous model employed a synthetic airway tree geometry, with the "nearest" bronchioles mapped by a simple planar ordering of the tree (see ref. Donovan (2016b) Fig. 1). Here we modify that approach for a full 3D tree geometry (Hedges et al., 2015); now the spatially dependent shear modulus is modelled via a scattered interpolant. Specifically the interpolant nodes are fixed at the terminal airway units, where the local inflation (and hence shear modulus) is known. Then linear interpolation is used within the Delaunay triangulation of the scattered sample points to determine inflation away from the terminal units. For the upstream airways, the shear modulus is computed by evaluation of the scattered interpolant (constructed from the order 1 airway computed as above.[6])
2. Airway parameters now vary not just with airway size but also account for structural heterogeneity (Pascoe et al., 2017). Specifically we have variation in the ASM area (M) and wall area (W). The statistical model of these parameters is described in the following section; here we consider only how they enter into the (dynamic) model equations. Specifically, the (normalized) ASM area alters the effective ASM pressure as $\hat{\kappa}_i = \kappa_i M_i$, while variation in the wall area W_i is accounted for geometrically (see Pascoe et al. (2017)).
3. The conducting airway tree is as used in Pascoe et al. (2017), obtained from Hedges et al. (2015) with central airways acquired from CT where feasible and with smaller airways generated with a space-filling algorithm which adheres to appropriate statistical properties (Tawhai et al., 2000).

[4] Although the system is now formulated only in terms of airway radius, with pressures and flows now implicit, these can be reconstructed via the algebraic constraints where needed for analysis of the results.

[5] This can easily be generalised to include a different number of neighbours (Donovan and Kritter, 2015).

[6] A note on computational efficiency: because the interpolant nodes do not change, only the data, it is best to use a form of the interpolant which readily allows for this.

2.2. Statistical model of inter-airway structural heterogeneity

The statistical model of inter-airway structural variation comes from Pascoe et al. (2017). A brief summary follows: first, the data are appropriately scaled to account for airway size (e.g. $\bar{M} = M(P_{bm})^{\alpha}$, where P_{bm} is the airway's basement membrane perimeter). The data, both unscaled and scaled, are shown in Fig. 2. Because the correlations between M and W are too great to be neglected, the rescaled data are then modelled as a bivariate log-normal distribution. The parameters for this bivariate log-normal distribution are fitted for both the data from control lungs, and from asthmatic lungs. Briefly, asthmatics have increased mean values for both M and W, compared with nonasthmatics, but similar variance and correlation. Full details are given in Pascoe et al. (2017). Using this statistical model, we generate a heterogeneous computational domain for the dynamic model. The parameter values for the bivariate log-normal fit are: for normal subjects $\mu_{\bar{W}} = -5.9$, $\mu_{\bar{M}} = -1.6$, $\sigma_{\bar{W}} = 0.60$, $\sigma_{\bar{M}} = 0.40$ and correlation 0.73 (for linear units in mm and areas in mm^2). For asthmatic subjects, $\mu_{\bar{W}} = -5.25$, $\mu_{\bar{M}} = -1.35$, $\sigma_{\bar{W}} = 0.56$, $\sigma_{\bar{M}} = 0.30$ and correlation 0.68 (Pascoe et al., 2017).

3. Results

3.1. Bimodal ventilation

We first demonstrate the qualitative emergence of clustered ventilation defects (Venegas et al., 2005b) and bimodal ventilation (Venegas et al., 2005a) in the asymmetric and heterogeneous domains specified by the airway tree geometry and statistical model of structural heterogeneity. A representative simulation is shown in Fig. 3; panel (a) gives a 3D representation of the parenchymal inflation; (b) shows the flow through individual airways, normalized to nominal flow; (c) shows the (bimodal) distribution of flow amongst the airways; and (d) shows the same data as (a), but here in a series of slices through the z-axis.

3.2. Functional implications of differences in inter-airway heterogeneity

To assess the functional implications of differences in inter-airway heterogeneity, we construct simulated dose response curves as given in Fig. 4. Simulated dose-response data is from 5 different randomized lung structures, for 3 different values of the coupling strength parameter A; given the 5 different levels of ASM activation (κ), the data shown are derived from 150 separate simulations. The ASM activation parameter κ is mapped to concomitant agonist dose using the human ASM data of Ijpma et al. (2015). Standard sigmoidal interpolants are fitted to the data points, as shown.

Naturally one expects that, given the increased mean values of both M and W in the asthma model (compared with control), markers of function would also show significant declines associated with these structural changes, and indeed the dose-response curve is shifted both up and left in response to the structural alterations. This shift in the dose-response curve is significant, yet somewhat modest. However some care should be taken in the interpretation – see the discussion for more details.

3.3. Airway-airway correlations and distributional assessment

The potential for bimodal ventilation distributions, clustered ventilation defects, and resulting paradoxical dilation (during agonist challenge) has been known now for some years (e.g. Venegas et al. (2005a, 2005b)). However, more recent advances, based on synchrotron phase-contrast CT, have allowed

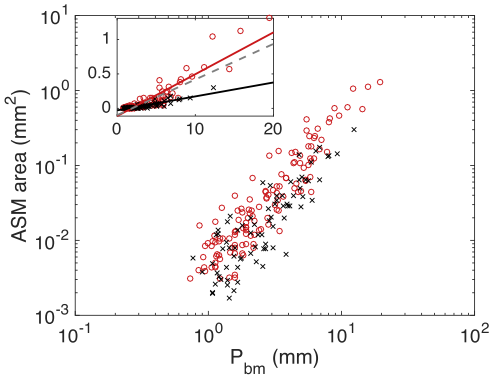

(a) Unscaled ASM area versus basement membrane perimeter (P_{bm}).

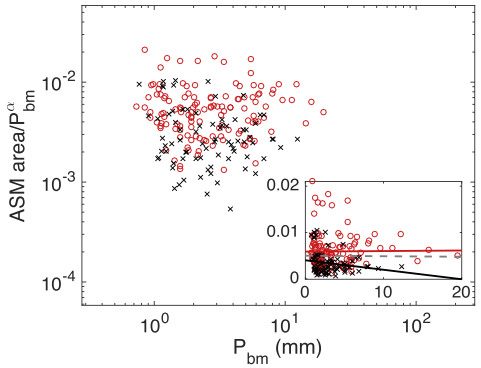

(b) Scaled ASM area versus basement membrane perimeter (P_{bm}). As in Pascoe et al.(2017), $\alpha = 1.875$.

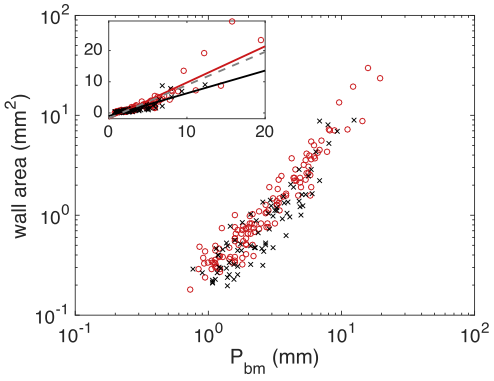

(c) Unscaled wall area versus basement membrane perimeter (P_{bm}).

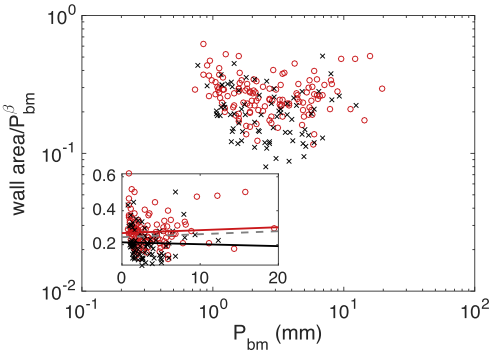

(d) Scaled wall area versus basement membrane perimeter (P_{bm}). As in Pascoe et al.(2017), $\beta = 1.47$.

Fig. 2. Experimental data on structural heterogeneity; data derived from human tissue histology, first published in Pascoe et al. (2017). Red circles (○) give data from asthmatic tissue; black x's (×) give data from non-asthmatic tissue. Main axes are given on a log-log scale; insets show the same data on a linear scale, with linear regressions for asthmatic (red, solid), non-asthmatic (black, solid) and combined (grey, dashed). See panel captions for individual descriptions. (For interpretation of the references to colour in this figure legend, the reader is referred to the web version of this article.)

much more detailed assessment of the distribution and heterogeneity of airway responses (Dubsky et al., 2017). Here we make comparisons between our simulated lungs and these measurements, in terms of heterogeneity and distribution of airway responses to agonist challenge. In Fig. 5, we show the heterogeneity of the airway response to agonist challenge in the simulated lung by plotting the baseline (pre-challenge) airway radius against the post-challenge (normalized) radius. Because the comparison experiments of Dubsky et al. (2017) were performed on mice, and the simulated lungs are human, quantitative comparisons are difficult; however, certain qualitative features are worth careful examination. First is that paradoxical dilation is apparent at all airway sizes, in both control and asthmatic simulated lungs. Dependence upon baseline airway size is primarily reflected by way of increased response heterogeneity in smaller airways; this response heterogeneity is broader in asthmatics than in controls.

The annotations in Fig. 5 are helpful for interpretation. The shaded grey area indicates the region which would be below the experimental detection threshold. The dashed line shows Friedman's super-smoother regression. Compared with the data of Dubsky et al. (2017), Friedman's super-smoother shows similar features for larger airways, but diverges sharply for the smallest airways. Several possible explanations arise for this apparent discrepancy: most likely is that it simply reflects a fairly modest shift in the dilation/contraction balance for small airways. Given the highly heterogeneous response across the airway population at that size, small shifts in the distribution can heavily impact estimates of the mean. It is also possible that airways below the experimental detection threshold are responsible for the shift, or that this is a species difference between mouse and human.

3.4. Direct comparison between control and asthmatic behaviour

One advantage of simulated lungs, over their experimental counterparts, is the ability to construct structurally-equivalent control and asthmatic structural domains. Specifically, the idea is that by seeding the pseudo-random number generator appropriately, we can generate structural lung domains which have the same structural heterogeneity *pattern*, yet which adhere to different statistical models (e.g. either control or asthmatic). That is, airways with particularly thick (or thin) ASM will occur in the same locations in each tree, though the exact quantitative values depend on the parameters of bivariate distribution. This is possible because the *type* of distribution is the same (bivariate log-normal), with alterations to the parameters only; if the underlying distributions were of different type, the simulations could not be matched in this way. All other model aspects remain fixed (e.g. A and κ are both fixed, and homogeneously applied) – thus the same dynamic

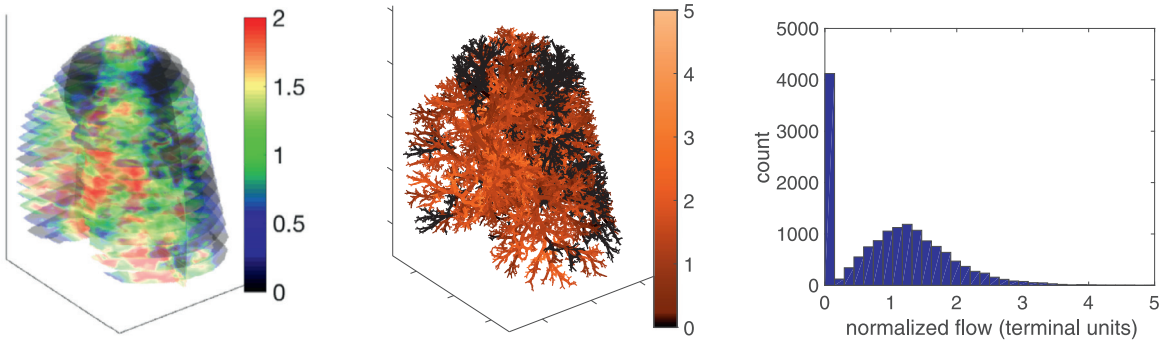

(a) 3D representation of parenchymal inflation.

(b) Flow through individual airways.

(c) Bimodal distribution of flow amongst the terminal airways.

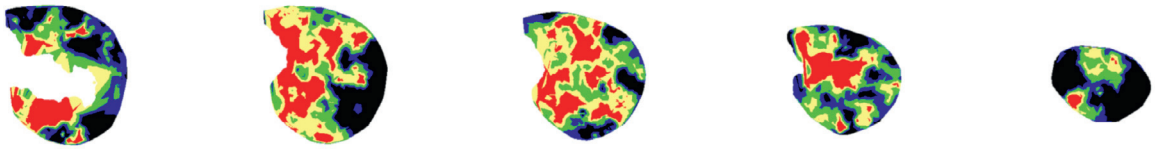

(d) Inflation field; z-slices. (Same colorbar as (a)).

Fig. 3. Qualitative emergence of clustered ventilation defects in an asymmetric and heterogeneous domain under agonist challenge. All panels normalized to homogeneous inflation/flow ($\hat{Q}$ in each terminal unit).

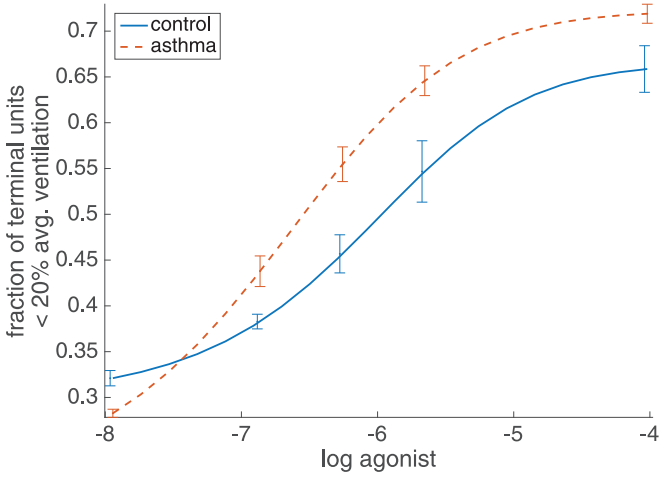

Fig. 4. Dose-response curves for fraction of terminal units with less than 20% normalized ventilation. Asthmatic structural heterogeneity clearly shifts the response relative to non-asthmatic structure. Error bars give standard error.

heterogeneity model is run on each of the matched structural domains. The results in Fig. 6 show such a comparison. One observation, apparent in Fig. 6(a), is that a type of paradoxical dilation is also present here: airways in the matched asthmatic lung may be either dilated or constricted relative to their control counterparts. As one might expect, this is also true of the flow through those airways (panel (b)). Panels (c) and (d) give the slice visualisations of flow in each case. While certain structures are preserved, due to the common branching structure and structural heterogeneity pattern, the alteration of airway properties does indeed substantially alter the flow patterns – even though the structural heterogeneity *pattern* is unchanged.

3.5. Correlations between remodelling and contraction/dilation

One obvious hypothesis is that there may be a correlation between pre-existing airway remodelling, and subsequent contraction/dilation during agonist challenge. As with the experimental data of Dubsky et al. (2017), however, the simulated lungs show remodelling properties of any single airway are not reliable predictors of dilation probability for that airway; this is true for either ASM area (M) or wall area (W). Typically the correlation coefficients are <0.05, with a maximum across all simulations of 0.095 vs M and 0.141 vs W. Plots of the relationship for these maximal correlation simulations are given in Fig. 7, and even in these selected simulations with highest correlation coefficient, there is no meaningful relationship. It is worth emphasising, however, that this is only *single airway* remodelling as a predictor of *single airway* contraction or dilation. It remains likely that structural heterogeneity of the *entire system* is an important determinant of contraction/dilation patterns, via interdependence and compensatory flow, and that the correlative influence of single airway properties are overwhelmed by the interdependence effects. However the exact nature of this relationship is yet unclear and remains an avenue of future investigation.

4. Discussion

In this paper we have considered a model of interaction between structural and dynamic heterogeneity during bronchoconstriction in both asthmatic and non-asthmatic simulated lungs. By doing so in a full human lung geometry, we are able to obtain insights into biological processes underpinning both asthmatic pathophysiology and control counterparts.

Specifically, we demonstrate the bimodal ventilation (Venegas et al., 2005a) and mixed airway contraction/dilation patterns long theorised (Venegas et al., 2005b) and recently shown

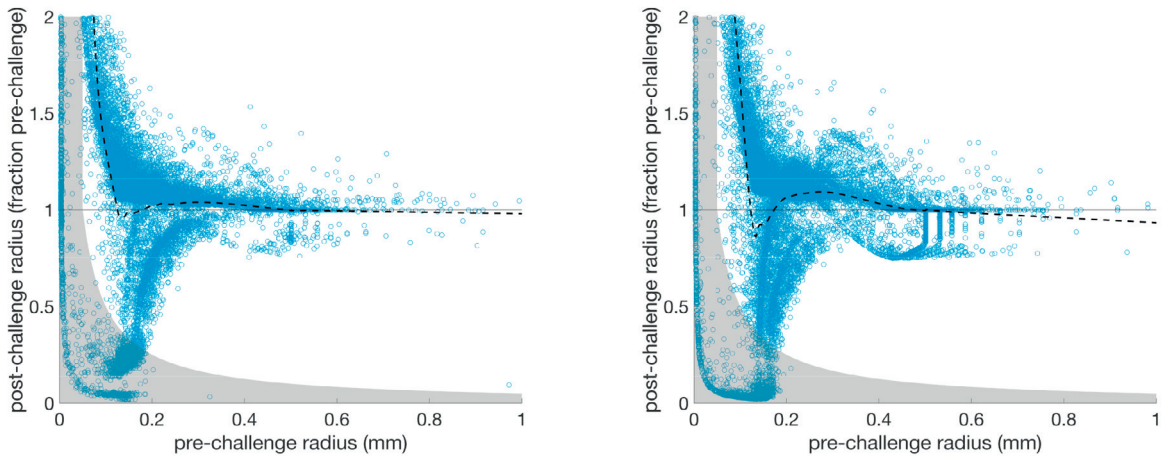

(a) Control (b) Asthma

Fig. 5. Distribution of airway calibre in response to simulated agonist challenge. Shaded grey area indicates areas which would be below the experimental detection threshold (Dubsky et al., 2017). Dashed line shows Friedman's super-smoother regression (Friedman, 1984) for comparison with Dubsky et al. (2017).

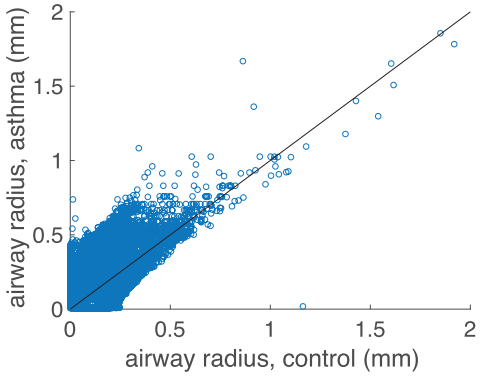

(a) Airway radius comparison, agonist challenged lungs. Control and asthmatic lungs with matched structural heterogeneity patterns.

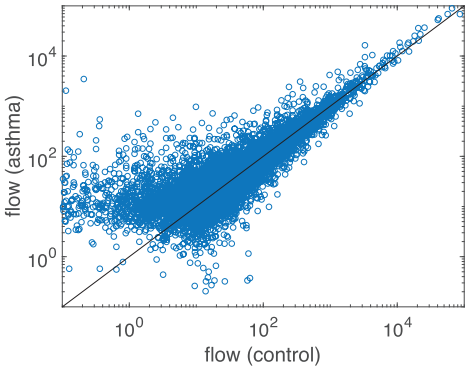

(b) Airway flow comparison, agonist challenged lungs. Control and asthmatic lungs with matched structural heterogeneity patterns. Note that the axis range excludes airways near closure for visibility.

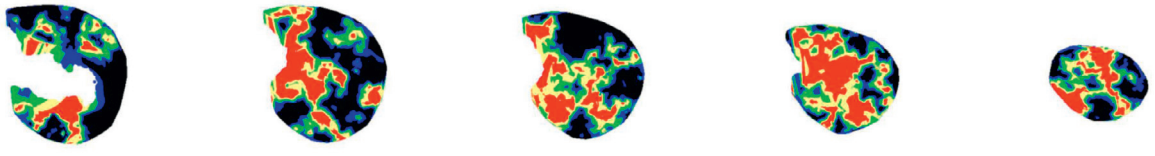

(c) Flow slices, control lung. Colorbar as in Fig. 3.

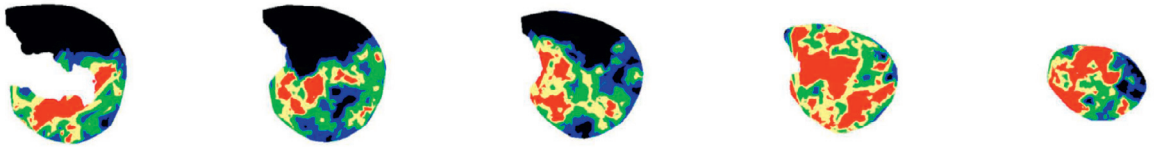

(d) Flow slices, asthmatic lung (structural heterogeneity pattern matched to control). Colorbar as in Fig. 3.

Fig. 6. Direct comparison between control and asthmatic matched simulated lungs.

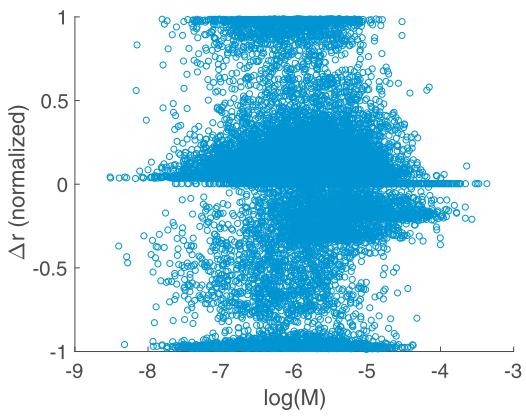

(a) Largest correlation simulation vs M; correlation 0.095.

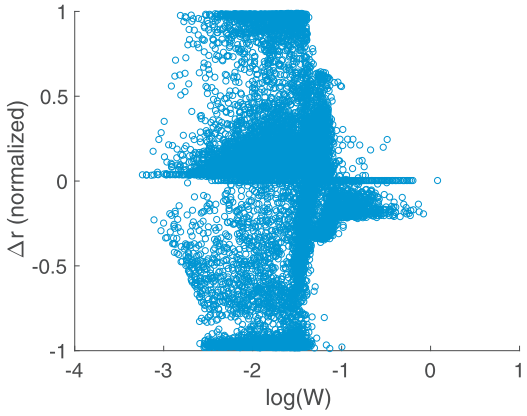

(b) Largest correlation simulation vs W; correlation 0.141.

Fig. 7. Selected simulations with largest correlations between remodelling and contraction/dilation. Note that typical correlation values are < 0.05.

experimentally (Dubsky et al., 2017); and moreover that both these ventilation patterns and resulting lung function are influenced by structural heterogeneity. We also compare contraction/dilation patterns between asthmatic and control simulated lungs and demonstrate the importance of the altered structure of asthmatic lungs, even for matched remodelling patterns. We also verify the finding of Dubsky et al. (2017) that the airway dilation probability is uncorrelated with the remodelling properties of that airway alone, though it remains likely that holistic remodelling patterns are critical determinants of contraction/dilation patterns. It is also worth noting that mixed contraction-dilation patterns persist in the absence of either structural heterogeneity or coupling via parenchymal tethering (e.g. $A = 0$), despite the fact that each of these does bring about significant change (for the former, magnitude of response to ASM activation; for the latter, changes to the spatial nature of the patterns).

Several important caveats should be kept in mind in the interpretation of these results. For example, in comparing the results of Section 3.3 (mixed-contraction dilation patterns) with those of Dubsky et al. (2017), one must bear in mind the imaging threshold (the shaded area of Fig. 5). Because of the significant number of simulated airways which lie in this region, it is possible both that the simulations agree very well with the experiments (if many experimental airways are also below threshold), or that there are fundamental, qualitative differences between the two (if there are few). Similarly, in assessing simulated lung function, model limitations preclude simulating a more exhaustive set of functional indicators (e.g. FEV1 (Hedges et al., 2015)). It is also worth noting that while clustered ventilation defects have been observed with a variety of imaging modalities (e.g. Simon et al. (2012)), there are important differences in what is being imaged; equally, the parenchymal inflation measure that we use here to visualize clustered ventilation defects (in fact, the scattered interpolant of terminal inflation) is a proxy for these visualization techniques and it is most suitable for qualitative, rather than quantitative, comparison.

In considering the magnitude of the dose-response curve shift, several things are worth bearing in mind: one, that it was not possible with this data to differentiate between the structural properties of subgroups within asthma (e.g. non-fatal asthma, or fatal asthma), and that splitting out by sub-group would likely reflect much larger differences. Furthermore, the measure here of low-ventilation units is a good direct measure from the model observables, but clinical measures such as resistance are highly nonlinear and thus might exhibit a much more pronounced shift.

This model draws upon the structural heterogeneity modelling of Lutchen and Gillis (1997), Thorpe and Bates (1997) and Pascoe et al. (2017), the dynamic heterogeneity work of Venegas et al. (2005b), Donovan and Kritter (2015) and Winkler and Venegas (2007, 2011, 2012), and more recent efforts to combine the two (Donovan, 2016b; Stewart and Jensen, 2015). Many different approaches are possible; some are summarized in these reviews (Donovan, 2011; Winkler et al., 2015), now several years old; more recent efforts include more detailed flow (Kim et al., 2015; Swan et al., 2012) and mechanics (Roth et al., 2017a; 2017b; 2017c; Yoshihara et al., 2017), though generally not in the conjunction with the airway dynamics needed for bronchoconstriction.

As with any model, understanding the assumptions is crucial for valid interpretation of the result. The assumptions used in the development of this model are discussed more fully in Section 2, and refs Donovan (2016b) and Pascoe et al. (2017). However, several deserve to be discussed more fully here, especially in the broader context of the literature. One key assumption is the vast simplification of airway smooth muscle dynamics, which are known to be complex (Bates, 2015; Donovan, 2013; Donovan et al., 2010; Mijailovich et al., 2000). In the same vein, the ASM is paired with idealized tube-law airways of Lambert et al. (1982) (as opposed to more detailed solid-mechanics models, e.g. Brook et al. (2010); Brook (2014)). Although the Lambert model has received recent experimental support in smaller airways Harvey et al. (2015), questions remain about its accuracy in the smallest airways (where much key behaviour occurs). Similarly, theoretical reproduction of experimental quasi-static pressure-radius curves (Gazzola et al., 2016) requires complexity not included here (Donovan, 2016a); even then, the exact mechanisms remain unclear.

In addition to the results presented in this paper, the model described herein provides a basis for theoretical examination of other hypothesized phenomena underpinning asthmatic pathophysiology. For example, the interactions of dynamic and structural heterogeneity on a whole lung scale provide a natural platform for theoretical studies of persistence of clustered ventilation defect location (de Lange et al., 2007; Svenningsen et al., 2014; Teague et al., 2014); the effect of spatial correlations in structural heterogeneity; or the (uncertain) mechanisms underlying therapeutic benefits of bronchial thermoplasty (Bonta et al., 2015; Laxmanan and Hogarth, 2015; Pretolani et al., 2014).

Acknowledgements

GMD gratefully acknowledges support from the Marsden Fund (Royal Society of New Zealand) (grant UOA1417).

Appendix A. Alveolar compliance

The treatment of alveolar compliance becomes

$$\hat{\boldsymbol{\alpha}} = \boldsymbol{\alpha} \circ \left(1 - \hat{c}\,\boldsymbol{\alpha}^{\circ -1} \circ \boldsymbol{r}^{\circ 4} \circ \boldsymbol{\nu}_{\downarrow}\right) \tag{A.1}$$

in terms of $\boldsymbol{\alpha}$, which is the vector form of the effective Poiseuille coefficients (using the notation of Donovan (2016b).) The parameter $\hat{c}$ then sets the effective compliance. Equivalently, in scalar form, we have

$$\hat{\alpha}_i = \begin{cases} \alpha_i(1 - \hat{c}\frac{r_i^4}{\alpha_i}), & \text{for } i \text{ an order 1 airway} \\ \alpha, & \text{otherwise.} \end{cases} \tag{A.2}$$

References

Anafi, R.C., Wilson, T.A., 2001. Airway stability and heterogeneity in the constricted lung. J. Appl. Physiol. 91 (3), 1185–1192.
Bates, J.H., 2015. Modeling the impairment of airway smooth muscle force by stretch. J. Appl. Physiol. 118 (6), 684–691.
Bonta, P.I., dHooghe, J., Sterk, P.J., Bel, E.H., Annema, J.T., 2015. Reduction of airway smooth muscle mass after bronchial thermoplasty: are we there yet? Am. J. Respir. Crit. Care Med. 191 (10), 1207–1208.
Brook, B., Peel, S., Hall, I., Politi, A., Sneyd, J., Bai, Y., Sanderson, M., Jensen, O., 2010. A biomechanical model of agonist-initiated contraction in the asthmatic airway. Respir. Physiol. Neurobiol. 170 (1), 44–58.
Brook, B.S., 2014. Emergence of airway smooth muscle mechanical behavior through dynamic reorganization of contractile units and force transmission pathways. J. Appl. Physiol. 116 (8), 980–997.
Donovan, G.M., 2011. Multiscale mathematical models of airway constriction and disease. Pulm. Pharmacol. Ther. 24 (5), 533–539.
Donovan, G.M., 2013. Modelling airway smooth muscle passive length adaptation via thick filament length distributions. J. Theor. Biol. 333, 102–108.
Donovan, G.M., 2016a. Airway bistability is modulated by smooth muscle dynamics and length-tension characteristics. Biophys. J. 111 (10), 2327–2335.
Donovan, G.M., 2016b. Clustered ventilation defects and bilinear respiratory reactance in asthma. J. Theor. Biol. 406, 166–175.
Donovan, G.M., Bullimore, S.R., Elvin, A.J., Tawhai, M.H., Bates, J.H., Lauzon, A.-M., Sneyd, J., 2010. A continuous-binding cross-linker model for passive airway smooth muscle. Biophys. J. 99 (10), 3164–3171.
Donovan, G.M., Kritter, T., 2015. Spatial pattern formation in the lung. J. Math. Biol. 1–31.
Dubsky, S., Zosky, G.R., Perks, K., Samarage, C.R., Henon, Y., Hooper, S.B., Fouras, A., 2017. Assessment of airway response distribution and paradoxical airway dilation in mice during methacholine challenge. J. Appl. Physiol. 122 (3), 503–510.
Friedman, J.H., 1984. A variable span smoother. Technical Report. DTIC Document.
Gazzola, M., Henry, C., Couture, C., Marsolais, D., King, G.G., Fredberg, J.J., Bossé, Y., 2016. Smooth muscle in human bronchi is disposed to resist airway distension. Respir. Physiol. Neurobiol. 229, 51–58.
Harvey, B.C., Parameswaran, H., Lutchen, K.R., 2015. Can breathing-like pressure oscillations reverse or prevent narrowing of small intact airways? J. Appl. Physiol. 119 (1), 47–54.
Hedges, K.L., Clark, A.R., Tawhai, M.H., 2015. Comparison of generic and subject-specific models for simulation of pulmonary perfusion and forced expiration. Interface Focus 5 (2), 20140090.
Ijpma, G., Kachmar, L., Matusovsky, O.S., Bates, J.H., Benedetti, A., Martin, J.G., Lauzon, A.-M., 2015. Human trachealis and main bronchi smooth muscle are normoresponsive in asthma. Am. J. Respir. Crit. Care Med. 191 (8), 884–893.
Kim, M., Bordas, R., Vos, W., Hartley, R.A., Brightling, C.E., Kay, D., Grau, V., Burrowes, K.S., 2015. Dynamic flow characteristics in normal and asthmatic lungs. Int. J. Numer. Methods Biomed. Eng. 31 (12).
Lai-Fook, S., 1979. A continuum mechanics analysis of pulmonary vascular interdependence in isolated dog lobes. J. Appl. Physiol. 46, 419–429.
Lambert, R., Wilson, T., Hyatt, R., Rodarte, J., 1982. A computational model for expiratory flow. J. Appl. Physiol. 52, 44–56.
de Lange, E.E., Altes, T.A., Patrie, J.T., Parmar, J., Brookeman, J.R., Mugler, J.P., Platts-Mills, T.A., 2007. The variability of regional airflow obstruction within the lungs of patients with asthma: assessment with hyperpolarized helium-3 magnetic resonance imaging. J. Allergy Clin. Immunol. 119 (5), 1072–1078.
Laxmanan, B., Hogarth, D.K., 2015. Bronchial thermoplasty in asthma: current perspectives. J. Asthma Allergy 8, 39.
Layachi, S., Porra, L., Albu, G., Trouillet, N., Suhonen, H., Peták, F., Sevestre, H., Suortti, P., Sovijärvi, A., Habre, W., et al., 2013. Role of cellular effectors in the emergence of ventilation defects during allergic bronchoconstriction. J. Appl. Physiol. 115 (7), 1057–1064.
Leary, D., Winkler, T., Braune, A., Maksym, G.N., 2014. Effects of airway tree asymmetry on the emergence and spatial persistence of ventilation defects. J. Appl. Physiol. 117 (4), 353–362.
Lui, J.K., Parameswaran, H., Albert, M.S., Lutchen, K.R., 2015. Linking ventilation heterogeneity quantified via hyperpolarized 3 he mri to dynamic lung mechanics and airway hyperresponsiveness. PLoS ONE 10 (11), e0142738.
Lutchen, K.R., Gillis, H., 1997. Relationship between heterogeneous changes in airway morphometry and lung resistance and elastance. J. Appl. Physiol. 83 (4), 1192–1201.
Mijailovich, S.M., Butler, J.P., Fredberg, J.J., 2000. Perturbed equilibria of myosin binding in airway smooth muscle: bond-length distributions, mechanics, and atp metabolism. Biophys. J. 79 (5), 2667–2681.
Pascoe, C.D., Seow, C.Y., Hackett, T.-L., Paré, P.D., Donovan, G.M., 2017. Heterogeneity of airway dimensions in humans: a critical determinant of lung function in asthmatics and non-asthmatics. Am. J. Physiol. Lung Cell. Mol. Physiol. ajplung–00421.
Pretolani, M., Dombret, M.-C., Thabut, G., Knap, D., Hamidi, F., Debray, M.-P., Taille, C., Chanez, P., Aubier, M., 2014. Reduction of airway smooth muscle mass by bronchial thermoplasty in patients with severe asthma. Am. J. Respir. Crit. Care Med. 190 (12), 1452–1454.
Roth, C.J., Becher, T., Frerichs, I., Weiler, N., Wall, W.A., 2017a. Coupling of eit with computational lung modeling for predicting patient-specific ventilatory responses. J. Appl. Physiol. 122 (4), 855–867.
Roth, C.J., Ismail, M., Yoshihara, L., Wall, W.A., 2017b. A comprehensive computational human lung model incorporating inter-acinar dependencies: application to spontaneous breathing and mechanical ventilation. Int. J. Numer. Methods Biomed. Eng. 33 (1).
Roth, C.J., Yoshihara, L., Ismail, M., Wall, W.A., 2017c. Computational modelling of the respiratory system: discussion of coupled modelling approaches and two recent extensions. Comput. Methods Appl. Mech. Eng. 314, 473–493.
Simon, B.A., Kaczka, D.W., Bankier, A.A., Parraga, G., 2012. What can computed tomography and magnetic resonance imaging tell us about ventilation? J. Appl. Physiol. 113 (4), 647–657.
Stewart, P.S., Jensen, O.E., 2015. Patterns of recruitment and injury in a heterogeneous airway network model. J. R. Soc. Interface 12 (111), 20150523.
Svenningsen, S., Guo, F., Kirby, M., Choy, S., Wheatley, A., McCormack, D.G., Parraga, G., 2014. Pulmonary functional magnetic resonance imaging: asthma temporal–spatial maps. Acad. Radiol. 21 (11), 1402–1410.
Swan, A.J., Clark, A.R., Tawhai, M.H., 2012. A computational model of the topographic distribution of ventilation in healthy human lungs. J. Theor. Biol. 300, 222–231.
Tawhai, M.H., Pullan, A., Hunter, P., 2000. Generation of an anatomically based three-dimensional model of the conducting airways. Ann. Biomed. Eng. 28 (7), 793–802.
Teague, W.G., Tustison, N.J., Altes, T.A., 2014. Ventilation heterogeneity in asthma. J. Asthma 51 (7), 677–684.
Tgavalekos, N.T., Musch, G., Harris, R., Melo, M.V., Winkler, T., Schroeder, T., Callahan, R., Lutchen, K., Venegas, J., 2007. Relationship between airway narrowing, patchy ventilation and lung mechanics in asthmatics. Eur. Respir. J. 29 (6), 1174–1181.
Thorpe, C.W., Bates, J.H., 1997. Effect of stochastic heterogeneity on lung impedance during acute bronchoconstriction: a model analysis. J. Appl. Physiol. 82 (5), 1616–1625.
Tzeng, Y.-S., Lutchen, K., Albert, M., 2009. The difference in ventilation heterogeneity between asthmatic and healthy subjects quantified using hyperpolarized 3he mri. J. Appl. Physiol. 106 (3), 813–822.
Venegas, J.G., Schroeder, T., Harris, S., Winkler, R.T., Melo, M.F.V., 2005a. The distribution of ventilation during bronchoconstriction is patchy and bimodal: a pet imaging study. Respir. Physiol. Neurobiol. 148 (1), 57–64.
Venegas, J.G., Winkler, T., Musch, G., Melo, M.F.V., Layfield, D., Tgavalekos, N., Fischman, A.J., Callahan, R.J., Bellani, G., Harris, R.S., 2005b. Self-organized patchiness in asthma as a prelude to catastrophic shifts. Nature 434 (7034), 777–782.
Winkler, T., Venegas, J.G., 2007. Complex airway behavior and paradoxical responses to bronchoprovocation. J. Appl. Physiol. 103 (2), 655–663.
Winkler, T., Venegas, J.G., 2011. Self-organized patterns of airway narrowing. J. Appl. Physiol. 110 (5), 1482–1486.
Winkler, T., Venegas, J.G., 2012. Are all airways equal? J. Appl. Physiol. 112 (9), 1431–1432.
Winkler, T., Venegas, J.G., Harris, R.S., 2015. Mathematical modeling of ventilation defects in asthma. Drug Discovery Today 15, 3–8.
Yoshihara, L., Roth, C.J., Wall, W.A., 2017. Fluid-structure interaction including volumetric coupling with homogenised subdomains for modeling respiratory mechanics. Int. J. Numer. Methods Biomed. Eng. 33 (4).